Generating Orbits for Stable Close Encounter Periodic Solutions of the Restricted Problem

Donald L. Hitzl*
Lockheed Palo Alto Research Laboratory, Palo Alto, Calif.

Recently the second species periodic solutions of the restricted three-body problem have been investigated in the limiting case $\mu = 0$. The term second species solution is due to Poincaré and is basically a Keplerian elliptical orbit about the large primary mass which, at some time, makes a close passage by the smaller attracting mass. Our new result is: for $\mu = 0$, second species orbits are critical if, and only if, the Jacobi Constant C has an extremum. This paper explains this new analytical result in some detail and relates it to the previous numerical determinations of stability.

Introduction

THE stability analysis of orbital motion is a problem of fundamental importance in celestial mechanics and dynamical astronomy. Especially intriguing is the stability analysis of periodic orbits for the planar restricted three-body problem. The existence of orbits which pass repeatedly near either the smaller, or both, of the two attracting masses (referred to as the Earth and the Moon in this paper) has now been firmly established.[1,2] Also, a significant amount of numerical work[3,4] has shown that, in general, these close encounter periodic orbits are highly unstable. However, an early theoretical stability analysis[5] was a failure, so the delicate but exceedingly important question of stability remained open.

Later, the use of matched asymptotic expansions[6] emerged as a powerful candidate technique for the analytical/numerical stability analysis of these periodic orbits. In fact, the primary motivation for extending the asymptotic matching formulas through $0(\mu^2)$ was to obtain a stability analysis valid through $0(\mu)$. Before this technique could be applied, however, a serious flaw remained – very few *stable* close encounter orbits were known.

Thus, to remedy this situation, the second species periodic solutions of the restricted three-body problem recently were investigated in the limiting case of $\mu = 0$. These solutions, called consecutive collision orbits by Hénon and generating orbits by Perko, form an infinite number of continuous one-parameter families. As a result of this analysis, an infinite number of limiting orbits now are known which are the correct generating solutions from which to start an analytical (and numerical) search for stable close encounter periodic solutions of the restricted problem for $\mu > 0$.

Periodic Orbits with Close Passages

During the last 10-15 years, the calculation of periodic orbits for the restricted three-body problem has been extensively pursued using high-speed digital (and even analog) computers. In fact, the desire to calculate accurate periodic orbits using the digital computer led to considerable advances in numerical integration techniques and algorithms (Refs. 7 and 8, for example). Previous to that time, the equations of motion were numerically integrated by hand. According to Szebehely, the most outstanding early example showing the importance of numerical experimentation is that of Elis Strömgren and the Copenhagen School. Their work was performed during the time 1913 to 1939 using the value $\mu = \frac{1}{2}$ almost exclusively. Another interesting early example is the case $\mu = 1/11$.[9]

In all of these numerical experiments, the investigators had one, or several, of the following goals in mind: 1) find families of periodic orbits, 2) calculate their stability, 3) determine the evolution of the family from beginning to end, and 4) infer general properties of the dynamical system from the behavior of a set of orbits. The natural beginning and natural termination (Ref. 10, pp. 486-487) of a family of periodic orbits can be at: 1) one, or both, of the primary masses μ and $1-\mu$, 2) one, or two, of the triangular libration points L_4 and L_5, and 3) infinity.

Then, following Szebehely, the natural end (or beginning) of a family of periodic orbits occurs when

$$E \triangleq (|C| + T + S)^{-1} \to 0 \tag{1}$$

since, corresponding to the three possibilities just specified: 1) the Jacobi constant $C \to \infty$, 2) the orbital period $T \to \infty$, and 3) the size of the orbit $S \to \infty$. Finally, we note that collision orbits do not, in general, terminate a family of periodic orbits. In fact, the collision orbits occurring in various families must be included as members of the family in order to continue the family of orbits to its proper termination.[10] Numerical integration of these collision orbits is accomplished by a transformation of both the independent (t) and dependent [$x(t)$, $y(t)$] variables to so-called regularized coordinates so that the singularities at the two primary bodies are removed.

As an example of the interplay between numerical calculations and theoretical analysis, the thesis of Roger Broucke in 1962 triggered Michel Hénon to begin a search for explanations of the observed types of motion and, in particular, to study the limiting orbits as $\mu \to 0$. Analyzing the numerical results obtained by Broucke, Hénon found that all the periodic orbits of the restricted problem found by Broucke approach one of the following three limiting forms as $\mu \to 0$:

1) Direct or retrograde circular orbits. These are the periodic orbits of the *first kind.*

2) Direct or retrograde elliptic orbits. These are the periodic orbits of the *second kind.*

3) Direct or retrograde consecutive collision orbits. These are the so-called periodic orbits of the *second species* and feature two collisions of the particle with the smaller primary mass during one period of the motion.

In fact, all of these limiting forms had been originally described by Poincaré.

Presented as Paper 76-840 at the AIAA/AAS Astrodynamics Conference, San Diego, Calif., Aug. 18-20, 1976; submitted Sept. 7, 1976; revision received June 17, 1977.

Index categories: Lunar and Interplanetary Trajectories; Spacecraft Navigation, Guidance, and Flight-Path Control.

*Research Scientist, Advanced Systems Studies Dept. Member AIAA.

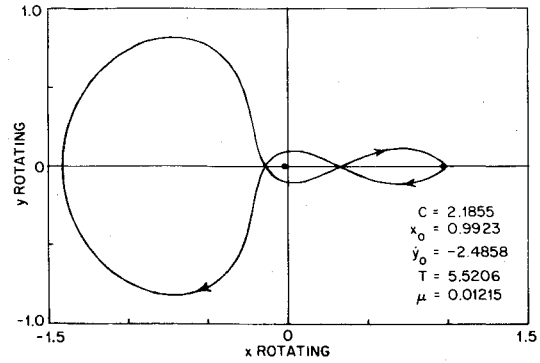

Fig. 1 A simple Earth-Moon periodic orbit plotted in the rotating coordinate system. This orbit is classified ratio $m/l = 1/2$, order $n = 1$ by Arenstorf; in the second species limit it is simply the direct orbit of family C_{12} located at $\tau/\pi = 1$, $\eta/\pi = 2$.

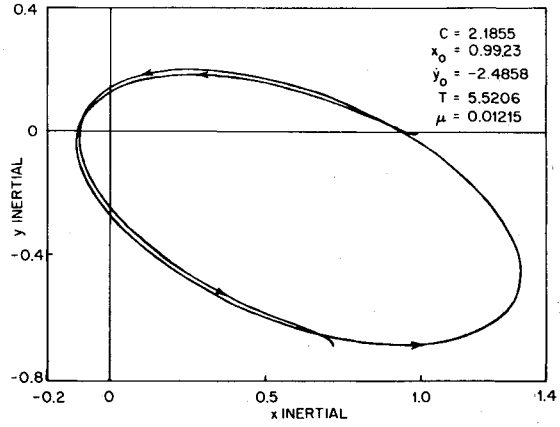

Fig. 2 The orbit shown in Fig. 1 plotted in an inertial coordinate system. The neighboring critical orbit in the second species limit $\mu = 0$ is shown in Fig. 10.

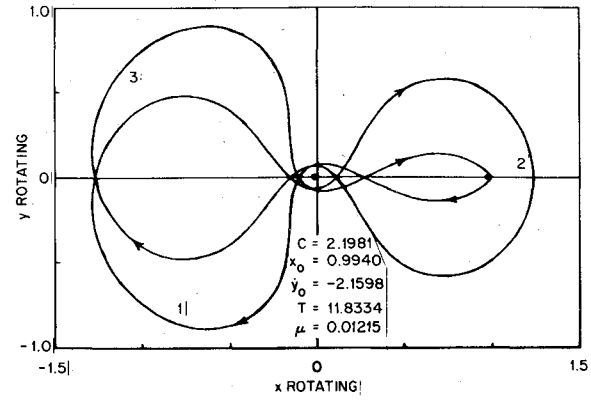

Fig. 3 A second Earth-Moon periodic orbit plotted in the rotating coordinate system. This orbit has $m/l = 1/2$, $n = 2$ and, in the second species limit, becomes the direct orbit of family C_{24} located at $\tau/\pi = 2$, $\eta/\pi = 4$.

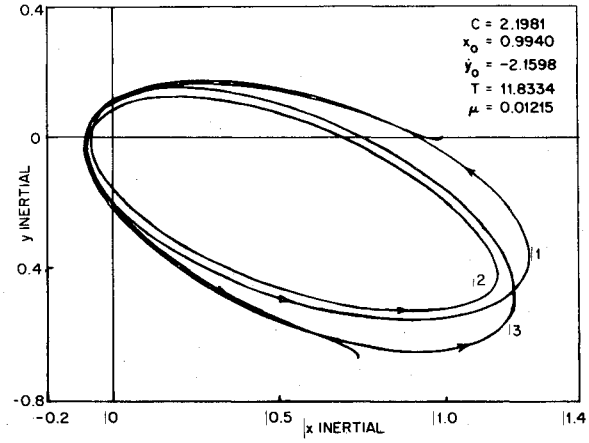

Fig. 4 The orbit of Fig. 3 redrawn in an inertial coordinate system. This orbit is similar to the critical second species limiting orbit $C_{24}(1)$ located at $\tau/\pi = 1.99362\ldots$, $\eta/\pi = 3.98751\ldots$.

However, as will be clearly seen later, consecutive collision orbits are the natural limit, as $\mu \to 0$, of second species orbits. Hence, consecutive collision orbits with $\mu = 0$ are the fundamental orbits to consider, if one wants to analyze close encounter orbits for small $\mu > 0$.

In general, the class of orbits of interest in this paper are *symmetric* periodic orbits for the value $\mu = 1/82.30 = 0.01215067\ldots \triangleq \mu^*$ appropriate to the Earth-Moon system. As shown in many of the figures, these periodic orbits are symmetric about the x axis of the rotating frame and feature, in particular, two perpendicular crossings of this axis.

To illustrate the type of periodic orbit categorized by the term "close encounter," two examples of such orbits are presented in Figs. 1-4. These are both direct orbits in an inertial (sidereal or fixed) frame while, in the rotating (synodic) coordinate system, the motion is always direct in the neighborhood of the Earth. The two orbits are shown in the rotating coordinate system in Figs. 1 and 3 and in an inertial frame in Figs. 2 and 4. Also, for the more complex orbit of Figs. 3 and 4, successive elliptical arcs traversed by the orbit are numbered 1 to 3.

These orbits originally were found by Arenstorf and his coworkers, Davidson and Causey. They came from Arenstorf's fundamental existence proof for solutions of the *second kind* with small $\mu > 0$. Furthermore, these solutions are the analytic continuations for small μ of appropriate Keplerian ellipses (generating orbits) in the limiting case $\mu = 0$. Arenstorf's orbits require that the *commensurability condition,*

$$|l|\, T_0 = m\ T_M = 2\pi m; \quad T_0 = 2\pi a^{3/2} \tag{2}$$

be satisfied at $\mu = 0$ for suitable relatively prime integers l and $m > 0$. (For direct orbits, $l > 0$ while, for retrograde orbits, $l < 0$). Here T_0 is the sidereal period of the orbit and T_M is the time for one revolution of the rotating frame which, by the standard normalization used in the restricted three-body problem, is 2π. Hence, the synodic period on the rotating ellipse is $2\pi m$.

Roughly, m is the number of orbits and partial orbits made by the Moon during the time that the particle makes $|l|$ revolutions (including, at most, one partial revolution) in its orbit. Thus, from Eq. (2),

$$a = |m/l|^{2/3} \tag{3}$$

and, for $m < |l|$,

$$1/2 < a < 1 \tag{4}$$

is required since, for the orbits of interest, the elliptic orbit of the particle must contain both masses. It is important to note that, for elliptic orbits of the second kind in the limit $\mu = 0$, the condition that $a^{3/2}$ is a rational number ($= m/l$) is required.

Orbits of this type are generally highly unstable. To illustrate, Fig. 5 shows a typical stability curve along a family of periodic orbits for $\mu > 0$. The orbital motion is stable in the interval $-1 < k < 1$; typically the curve $k(x_0)$ attains positive and negative values several orders of magnitude removed from this stable band. However, the primary motivation for the recent studies was the desire to find, if possible, stable close encounter orbits for the value μ^* corresponding to the Earth-Moon system. This seemed at first to be an impossible task and probably would not have been attempted except for

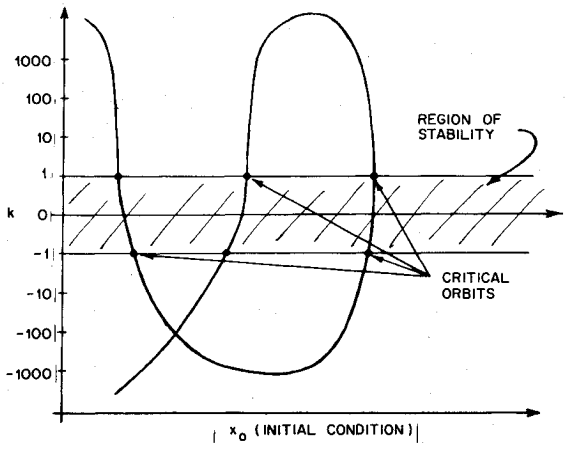

Fig. 5 The typical behavior of the stability index k along a given family of second species orbits of the restricted problem for $\mu > 0$. As $\mu \to 0$, the maximal values for $|k| \to \infty$ and the slope $\partial k/\partial x_0$ becomes generally steeper. In the limit $\mu = 0$, the entire locus for k is at $\pm\infty$ with occasional jumps from one side to the other at isolated critical orbits possessing extremal values for C.

the existence of one further piece of numerical evidence – the exceptional orbits $m1$ and $m2$ found by Hénon and Guyot in 1969 and described in the next section.

A Single Exceptional Orbit

In the late 1960's Hénon and his co-worker Guyot set the following task for themselves. Find the *critical* periodic orbits for six particularly important (and simple) families for all values of μ ($0 \leqq \mu \leqq 1$). Critical periodic orbits are those for which the stability index k (called a by Hénon) has either of the values ± 1; as shown in Fig. 5, these are then the bounding orbits, along the family, for a set of stable periodic orbits. The orbits they considered were the retrograde and direct orbits about either, or both, of the two primary bodies. Furthermore, the orbits were, for the most part, *simple-periodic*, so that the periodic orbit closes on itself after only two crossings of the x axis in the rotating frame. The appearance of the two exceptional critical orbits $m1$ and $m2$ is shown in Fig. 6. These orbits belong to the family m of retrograde simple-periodic orbits about both primaries (Strömgren's notation).

For small values of μ, the orbits are actually stable between the critical orbits $m1$ and $m2$. Utilizing data from their paper (Ref. 11, pp. 367-368), the graph given in Fig. 7 was prepared. This figure depicts the very narrow domain of stability for these "close encounter" orbits. As $\mu \to 0$, the two orbits $m1$ and $m2$ coalesce to a single limiting orbit termed a *critical generating orbit*. Furthermore, this limiting orbit was known to correspond to a particular member of family A_0 of consecutive collision orbits which, moreover, attained a local maximum for the Jacobi constant C.[11]

The orbital motion corresponding to the critical orbit $m1$ is further illustrated in Fig. 8. Here, using the Earth-Moon mass ratio μ^*, five complete orbits are traced out in the inertial frame.

Knowing these facts, we then set out to find further critical generating orbits since it was not expected that this single family of orbits was the only example exhibiting such behavior. However, before discussing this analysis, the general problem of stability analysis of periodic orbits will be described briefly in the following section.

Stability of Periodic Orbits

Usually stability of a periodic orbit is evaluated numerically using one of two generally accepted methods. These are 1) the

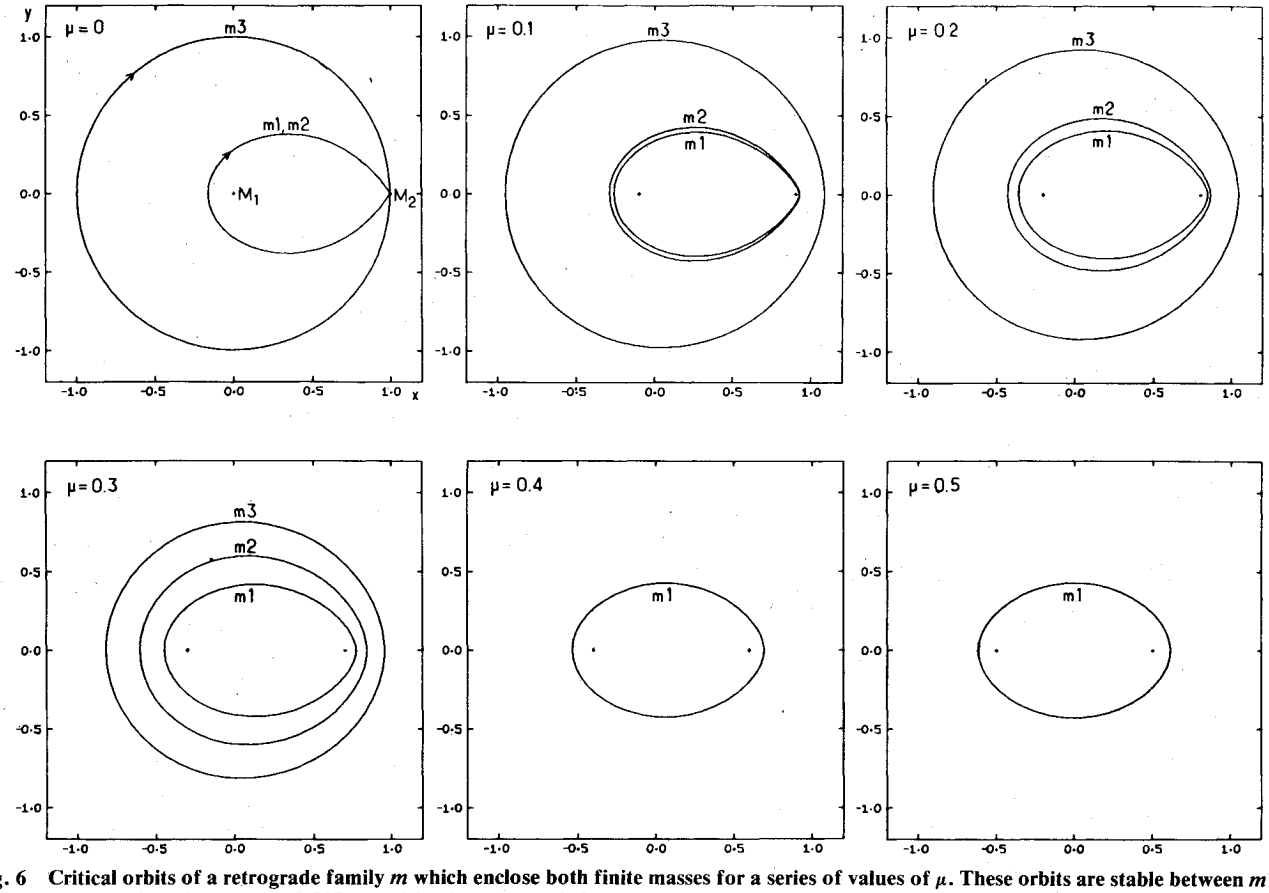

Fig. 6 Critical orbits of a retrograde family m which enclose both finite masses for a series of values of μ. These orbits are stable between $m1$ and $m2$ and outside $m3$ for $0 < \mu < \mu_0 = 0.327\ldots$ and for $1 - \mu_0 < \mu < 1$; for $\mu_0 < \mu < 1 - \mu_0 < 1 - \mu_0$, the orbits are stable outside $m1$. Otherwise, the orbits are unstable. (From Ref. 11, p. 354).

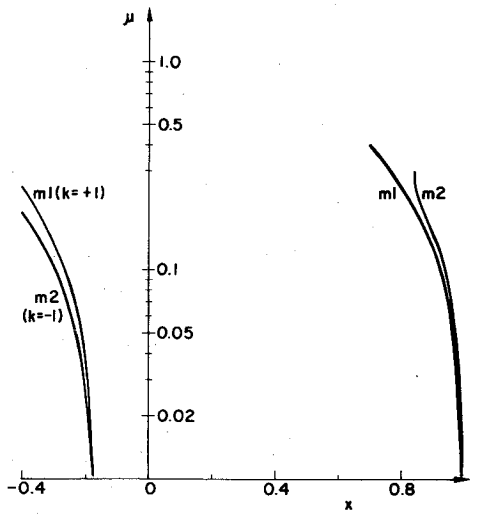

Fig. 7 The domain of stability for $\mu \geq 0$ for the close encounter orbits of family *m*. The single limiting orbit at $\mu = 0$ is the critical second species generating orbit labelled $A_0(-1)$.

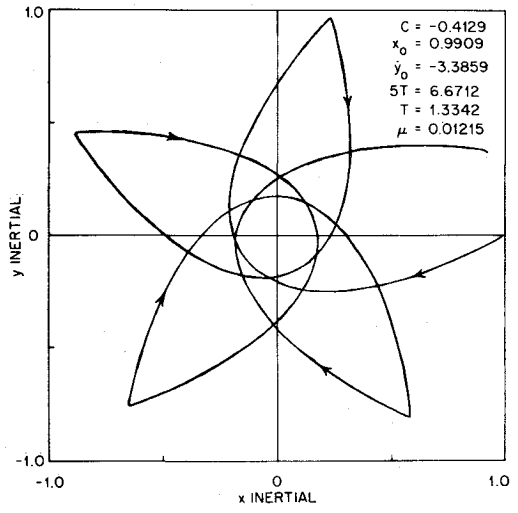

Fig. 8 Five complete orbits for the critical retrograde member *m*1 of family *m* shown in an inertial coordinate system.

method of displaced orbits and 2) integration of the linear variational equations. It should be pointed out that, for both techniques, only the linear, or infinitesimal, stability of the orbit is determined.

The first approach[11] consists in numerically evaluating the partial derivatives $\partial x(T)/\partial x_0$, $\partial x(T)/\partial \dot{x}_0$, etc., by computing the effect on the periodic orbit of small perturbations, δx_0 and $\delta \dot{x}_0$, in the initial conditions. In particular, for *symmetric* periodic solutions, only one-half of the periodic orbit is needed; hence, letting x_1 and $\dot{x}_1$ denote the values at the second perpendicular crossing of the x axis at $t = T/2$, the four sensitivities

$$A = \frac{\partial x_1}{\partial x_0}, \quad B = \frac{\partial x_1}{\partial \dot{x}_0}, \quad C = \frac{\partial \dot{x}_1}{\partial x_0}, \quad D = \frac{\partial \dot{x}_1}{\partial \dot{x}_0} \tag{5}$$

are obtained. The stability index k then is defined by

$$k = AD + BC \tag{6}$$

and, excluding resonances discussed in the foregoing, we have stability for $|k| < 1$, instability for $|k| > 1$, and critical periodic orbits located on the stability boundary for $|k| = 1$.

This method is seen to be quite simple and straightforward; in particular, no additional differential equations have to be numerically integrated. However, to insure that the values of k are indeed accurate, some care must be taken as follows:

1) The orbits need to be integrated in double precision to an accuracy of $\sim 10^{-14}$.

2) The exact numerical values for the initial perturbations δx_0 and $\delta \dot{x}_0$ should be chosen carefully.

3) Symmetrically perturbed orbits should be calculated. Then the derivative of $f(x)$ is obtained from

$$[f(x+h) - f(x-h)]/2h$$

and *not* from

$$[f(x+h) - f(x)]/h$$

4) The two-dimensional perturbations, $\delta x(t)$ and $\delta \dot{x}(t)$, satisfy the area-preserving property

$$AD - BC = 1 \tag{7}$$

of a Hamiltonian system. This quantity should be monitored as it provides a very sensitive accuracy test.

The second approach involves numerically integrating the linear variational equations. These equations can be written

$$\dot{\xi} = A\xi \tag{8}$$

where $\xi \triangleq (\delta x, \delta y, \delta \dot{x}, \delta \dot{y})^T$ is a 4×1 vector of position and velocity perturbations and A is a 4×4 matrix of the form

$$A = \begin{bmatrix} 0 & I_2 \\ F_2 & 0 \end{bmatrix} \tag{9}$$

where I_2 is the 2×2 identity matrix and F_2 is a 2×2 symmetric matrix whose elements depend upon the nominal periodic solution $[x(t), y(t)]$ under study. The solution of Eq. (8) then gives the behavior of small perturbations from the nominal periodic motion.

By successively perturbing each of the four elements (states) in ξ, a fundamental matrix R (sometimes called the monodromy matrix) is determined from

$$\dot{R} = AR; \quad R(t_0) = I_4 \tag{10}$$

so that the columns of R are four linearly independent solutions of the variational equations. (Note that, for a problem with two degrees of freedom, 16 additional equations must be numerically integrated).

For autonomous Hamiltonian systems of two degrees of freedom, the eigenvalues of R have the form

$$1 \quad 1 \quad \lambda \quad 1/\lambda \tag{11}$$

with

$$\begin{aligned} \lambda &= e^{\alpha T} \\ \alpha &= \text{characteristic exponent} \\ T &= \text{orbit period} \end{aligned} \tag{12}$$

The trace Tr of R is simply

$$Tr = 2 + \lambda + 1/\lambda = 2 + 2 \cosh \alpha T \tag{13}$$

and the stability index k given in Eq. (6) is

$$k = \tfrac{1}{2}(Tr - 2) = \cosh \alpha T \tag{14}$$

Note that, for $k = +1$, $Tr = 4$, and all four eigenvalues, $\lambda = 1$ so $\alpha = 0$. Also, for $k = -1$, $Tr = 0$, and $\lambda = -1$ so $\alpha = i\pi/T$. Hence, for stability, we have $0 < Tr < 4$ corresponding to $-1 < k < 1$, and then α is purely imaginary so $\alpha \triangleq i\beta$ giving $\lambda = e^{i\beta T} = \cos\beta T + i \sin\beta T$, and $k = \cos\beta T$.

It is convenient to visualize the roots λ as travelling around the unit circle in the complex plane. Then, if two roots $\lambda = -1$, there is a 2:1 resonance at the lower stability boundary ($k=-1$) since there are always two eigenvalues $+1$ for a Hamiltonian system. Furthermore, periodic orbits also can be unstable at the particular values $k=-\frac{1}{2}$ and $k=0$ corresponding to $\beta T=2\pi/3$ and $\beta T=\pi/2$, respectively. These cases of 3:1 and 4:1 resonance then require a finer analysis. In general, instability is to be expected for the 3:1 resonance whereas, at the 4:1 resonance, either stability or instability is possible depending upon the nonlinearities.

Critical Generating Orbits

In general, orbits with consecutive collisions are "infinitely unstable" with a stability index $k=\pm\infty$. However, following a family of consecutive collision orbits, we find that the Jacobi constant C varies continuously and occasionally passes through extremal values. Furthermore, previous work on critical orbits for the restricted problem[4] showed that, along a family of periodic orbits, an orbit with an extremal value in C *must be* a critical orbit with $k=+1$. Hence, by determining consecutive collision orbits with extrema in C for the limiting case of $\mu=0$, isolated orbits possessing jumps in the stability index k from $\pm\infty$ to $\mp\infty$ are obtained. These critical generating orbits are thus of great interest since, for small $\mu>0$, k will only reach very large values (rather than infinite values) and the transitions across the stable region $-1\leqq k\leqq 1$ now will occur over a finite (but small) interval. As a result, two critical orbits with $k=+1$ and $k=-1$, respectively, will be obtained which separate a small interval of stable orbits from the remaining orbits, which are generally strongly unstable.

As mentioned previously, the particular set of periodic solutions which have been studied are the so-called second species orbits in the limit $\mu=0$. This general case is described as follows. The Earth (mass 1) is located at the origin of an inertial $x\,y$ coordinate system and the Moon (mass 0) describes a circular orbit of radius 1. A massless particle also orbits in the same plane as the Moon along an elliptical path in either a direct or retrograde sense. At $t=0$, the Moon is located at $x=1$, $y=0$ and the particle is located on the x axis either at perigee or apogee. Thus, to incorporate all the possibilities, the following "switch functions" σ_i are defined.

$$\sigma_0=\begin{cases}+1\\-1\end{cases}\quad\text{if perigee is located at}\quad x\begin{cases}>0\\<0\end{cases}\tag{15a}$$

$$\sigma_1=\begin{cases}+1\\-1\end{cases}\quad\text{if the orbit is}\quad\begin{cases}\text{direct}\\\text{retrograde}\end{cases}\tag{15b}$$

$$\sigma_2=\begin{cases}+1\\-1\end{cases}\quad\text{if the particle is located at}\quad\begin{cases}\text{perigee}\\\text{apogee}\end{cases}\quad\text{at } t=0\tag{15c}$$

Finally, the two collisions of the particle and (massless) Moon occur at the symmetrical times $t=-\tau$ and $t=\tau$, respectively, with

$$x(\tau)=x(-\tau)\tag{16a}$$

$$y(\tau)=-y(-\tau)\tag{16b}$$

so the collision points (P and Q) are symmetrical with respect to the inertial x axis.

In these inertial coordinates, the Moon's position is simply given by

$$x=\cos t\tag{17a}$$

$$y=\sin t\tag{17b}$$

while the particle's location is expressed in terms of the eccentric anomaly E as follows

$$x=\sigma_0 a(\sigma_2\cos E-e)\tag{18a}$$

$$y=\sigma_0\sigma_1\sigma_2 a\sqrt{1-e^2}\sin E\tag{18b}$$

with Kepler's equation for the time

$$t=a^{3/2}(E-\sigma_2 e\sin E)\tag{19}$$

Note the appearance of the three switch functions so that all of the possible initial conditions are accommodated in one equation set. Furthermore, the "classical" eccentric anomaly E, measured from perigee, has been generalized so that $E=0$ either at perigee ($\sigma_2=+1$) or at apogee ($\sigma_2=-1$).

Specializing Eqs. (18) and (19) now to the second collision at point Q with $t=\tau$ and $E=\eta$ gives

$$c_\tau=\sigma_0 a(\sigma_2 c_\eta-e)\tag{20a}$$

$$s_\tau=\sigma_0\sigma_1\sigma_2 a\sqrt{1-e^2}\,s_\eta\tag{20b}$$

$$\tau=a^{3/2}(\eta-\sigma_2 e\,s_\eta)\tag{20c}$$

where the abbreviations $s_x=\sin x$, $c_x=\cos x$ have been employed. From symmetry, the same equations are obtained at point P where $t=-\tau$ and $E=-\eta$. Consequently, we have a system of three equations in the four unknowns τ, η, a, e, and thus an infinity of solutions.

Eliminating the orbit elements a and e from Eq. (20), a timing condition $F_0(\tau,\eta;\sigma,\sigma_\eta)=0$ for consecutive collision orbits can be obtained where $\sigma\triangleq\sigma_0\sigma_2$ and $\sigma_\eta\triangleq\operatorname{sgn}(\sin\eta)$. With the additional definition

$$\rho\triangleq\sigma_\eta\sqrt{1-\sigma\,c_\tau c_\eta}=\sqrt{a}\,s_\eta\tag{21}$$

this condition is

$$F_0(\tau,\eta;\sigma,\sigma_\eta)=\rho[\eta\rho^2-s_\eta(c_\eta-\sigma c_\tau)]-\tau s_\eta^3=0\tag{22}$$

Equation (22) originally was derived and resolved numerically by Hénon; he found an infinite number of continuous one-parameter families of solutions. Also these solutions had an unexpected richness and variety. The results of his calculations are shown in Fig. 9, where the characteristics (the loci of suitable initial conditions) for various families (labelled A_0, A_1, A_2, ..., B_1, B_2, ..., C_{12}, C_{23}, ...) of orbits are plotted as a function of the variables τ and η. Only a part of the τ, η plane is shown; in fact, solutions exist for all values of $\tau>0.51500\ldots$ and $\eta>0$. This plane has distinct advantages, for we see that the characteristics are neatly separated and form easily recognizable patterns. On the other hand, in the a, e plane the loci are hopelessly entangled so that the plot is virtually impossible to work with (Ref. 12, Fig. 9).

Now, we want to comment on the somewhat strange limit for the second species solutions as $\mu\to 0$. It seems necessary to point out that in the limit $\mu=0$, one does not fall back to periodic solutions of the first or second kind of the two-body problem. For this particular type of orbit, as μ tends to zero, the distance of closest approach d to the second body also goes to zero in such a way that, for $\mu=0$, a finite value of μ/d is obtained! This is somewhat paradoxical for it means that, even when the second body has *no* mass ($\mu=0$), the effect of the second body is *not* negligible. Thus, as is known (Ref. 12, p. 393, Ref. 13, Chap. 32) consecutive collision orbits are the natural limit of second species periodic orbits of the restricted problem as $\mu\to 0$.

The only algebraic integral in the restricted problem is the Jacobi integral

$$x^2+y^2+\frac{2(1-\mu)}{r_1}+\frac{2\mu}{r_2}-\dot{x}^2-\dot{y}^2=C\tag{23}$$

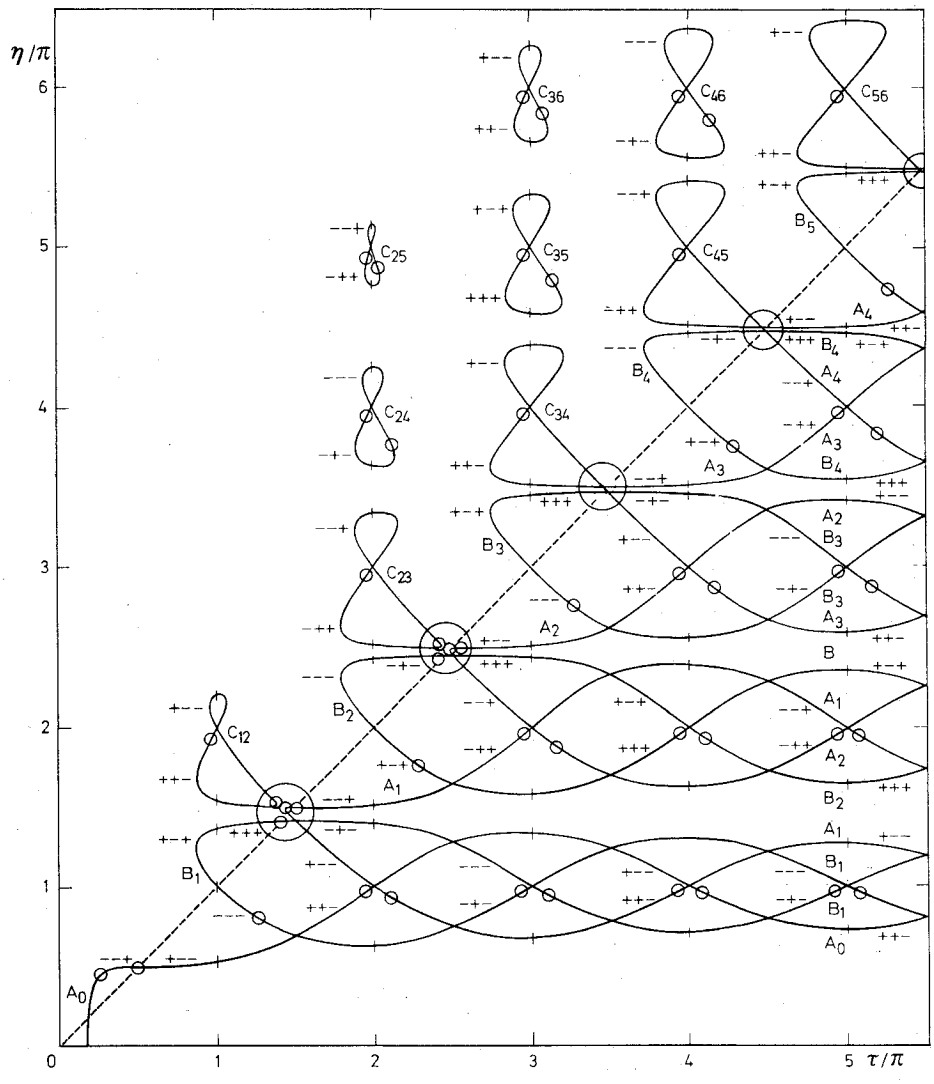

Fig. 9 Characteristics for several families of consecutive collision orbits shown in the τ, η plane (from Ref. 12). The approximate location of 62 critical orbits is denoted by a small circle on the characteristics; these locations, however, are somewhat exaggerated for clarity. The three signs are for σ_0, σ_1, and σ_2, respectively.

where C is the Jacobi constant. This can also be written

$$C=2(h_z-E) \tag{24}$$

expressing the well-known result that the total energy E and the z component of angular momentum h_z are conserved in the combination h_z-E. Using the equations

$$E=-1/2a \tag{25a}$$

$$h_z=\sigma_1\sqrt{a(1-e^2)} \tag{25b}$$

from the two-body problem gives

$$C=2\sigma_1\sqrt{a(1-e^2)}+1/a \tag{26}$$

Note that Eq. (26), expressing C as a function of a and e, is meaningful for any elliptical orbit (second species or not). Restricting ourselves now to second species solutions, C assumes the remarkably simple form

$$C(\tau,\eta;\sigma,\sigma_\eta)=\frac{2\sigma s_\tau}{\rho}+\frac{s_\eta^2}{\rho^2} \tag{27}$$

in the limiting case of $\mu=0$. Consecutive collision orbits located at extremal values of C now can be obtained *analytically* as follows. The orbit must be located at an extremal value of C together with the constraint that the orbit also satisfies the timing condition $F_0=0$ of Eq. (22). Thus we set

$$\frac{\partial}{\partial\tau}[C(\tau,\eta)+\lambda F_0(\tau,\eta)]=0 \tag{28a}$$

$$\frac{\partial}{\partial\eta}[C(\tau,\eta)+\lambda F_0(\tau,\eta)]=0 \tag{28b}$$

yielding an equation

$$G\triangleq C_\tau F_{0_\eta}-C_\eta F_{0_\tau}=0 \tag{29}$$

after the unknown Lagrange multiplier λ is eliminated. This equation is

$$G^*(\tau,\eta;\sigma,\sigma_\eta)\triangleq\sigma\frac{\rho^4}{s_\eta^2}G=\rho[T_1c_\eta^2+T_2c_\eta+T_3]$$
$$+c_\tau c_\eta^4-2\sigma c_\eta^3+2c_\tau c_\eta^2-\sigma c_\tau^2(3-c_\tau^2)c_\eta+c_\tau(2-c_\tau^2)=0 \tag{30}$$

where the T_i contain the secular terms in τ. The desired critical orbits then correspond to the intersection of the loci $F_0=0$ and $G^*=0$.[14]

However, the key result is that the infinite set of extremal orbits possessing jumps in the stability index k is now accessible analytically and, since it is known that an extremum in C along a periodic family must be a critical orbit with $k=+1$, we thus have a *sufficient* condition for an orbit to lie on the boundary of stability.

Direct Stability Analysis

Consider the second of the five orbits in Fig. 8 for the critical orbit $m1$. Using this figure, the five times t_{-2}, t_{-1}, t_0, t_1, and t_2 are defined by

t_{-2} = time of previous encounter with the Moon
t_{-1} = time of previous departure from the Moon
t_0 = time of perigee passage near the Earth
t_1 = time of next encounter with the Moon. Setting the midpoint $t_0 = 0$, we have $t_1 = -t_{-1} > 0$
t_2 = time of next departure from the Moon

Now, in the neighborhood of the Moon for $\mu > 0$, the orbital motion is along a hyperbola. We have

v_∞ = relative velocity at "infinity" on the osculating Moon-centered hyperbola
b = perpendicular distance from the Moon to the hyperbolic asymptote; also called the impact parameter
e_H = eccentricity of the hyperbolic passage around the Moon ($e_H > 1$)
t_p = time of perigee passage for the osculating hyperbolic motion
r_p = perigee radius at the Moon
v_p = relative velocity at lunar perigee
α = angular position (measured counterclockwise) of the relative velocity vector v_∞
δ = $\alpha_2 - \alpha_1 = \alpha_{-1} - \alpha_{-2}$ = angular deflection of v_∞ during the hyperbolic passage

Then, for the Moon-centered hyperbola, the following equations apply:

$$r_p v_p = b v_\infty \quad \text{(conservation of angular momentum)} \tag{31a}$$

$$e_H^2 = 1 + v_\infty^4 4b^2/\mu^2 \tag{31b}$$

$$r_p = \frac{\mu}{v_\infty^2}(e_H - 1) = b\sqrt{\frac{e_H - 1}{e_H + 1}} \tag{31c}$$

$$\delta = 2\sin^{-1}(1/e_H) \tag{31d}$$

Finally, in order to evaluate the stability of a close encounter orbit, the perturbation vector $\boldsymbol{P}$ is defined

$$\boldsymbol{P} \triangleq \begin{bmatrix} dt_p \\ db \\ dv_\infty \\ d\alpha \end{bmatrix} \tag{32}$$

for small changes in the hyperbolic parameters describing the motion near the Moon.

By differentiating the appropriate formulas obtained from the first-order theory of asymptotic matching, a "recurrence relation" connecting the perturbations at t_{-1} and t_1 can be obtained.[15] We write

$$\boldsymbol{P}_1 = T\boldsymbol{P}_{-1} \tag{33}$$

where the matrix elements T_{mn} are of the general form

$$T_{mn} = \hat{i}_1^T \Phi_{\alpha\beta}(t_1, t_{-1})\hat{j}_{-1} \tag{34}$$

with

$\hat{i}_1$ = direction of the relative velocity V_1 on the unperturbed conic at $t = t_1$
$\hat{j}_1$ = $\hat{k} \times \hat{i}_1$ = direction normal to V_1
$\Phi_{\alpha\beta}$ = a 2×2 submatrix (Φ_{rv} for example) of the 4×4 state transition matrix $\Phi(t_1, t_{-1})$

For the interested reader, full details are available elsewhere.[16]

Next, including the hyperbolic passage around the Moon from t_1 to t_2, v_∞ is rotated through the angle δ so, from Eq. (31d),

$$d\alpha_2 = d\alpha_1 - \frac{4\sqrt{e_H^2 - 1}}{V e_H^2} dv_{\infty_1} - \frac{2V^2}{\mu e_H^2} db_1$$

$$\triangleq d\alpha_1 + h_1\, dv_{\infty_1} + \frac{h_2}{\mu} db_1$$

giving the following "recurrence relation" from t_{-1} to t_2

$$\boldsymbol{P}_2 = M\boldsymbol{P}_{-1} \tag{36}$$

i.e., over a complete period of the motion. Note the appearance of the "dangerous terms" with μ^{-1} as a factor. Also, from Eq. (23), the relative velocity V on the unperturbed ellipse has the value

$$V = \sqrt{3 - C} \tag{37}$$

at the collision.

Stability is determined by the trace of M; we have

$$Tr = \sum_{i=1}^{4} M_{ii} = \sum_{i=1}^{4} T_{ii} + h_1 T_{34} + \frac{h_2}{\mu} T_{24} \tag{38}$$

where, for stability, $0 < Tr < 4$. Hence, as $\mu \to 0$, the matrix element

$$\frac{\partial b_1}{\partial \alpha_{-1}} = T_{24} = M_{24} = \frac{\partial b_2}{\partial \alpha_{-1}} \tag{39}$$

must vanish for stability so

$$S \triangleq -V\, T_{24} = V^2 \hat{j}_1{}^T \Phi_{rv}(t_1, t_{-1})\hat{j}_{-1} = 0 \tag{40}$$

is a *necessary* stability condition for second species orbits in the limit $\mu = 0$.[16] A *nontrivial* algebraic reduction of Eq. (40) then gives

$$\tfrac{1}{2}\, \sigma \rho s_\eta^2 S \equiv G^* = 0 \tag{41}$$

so, to within these multiplicative factors, the conditions we have obtained are both necessary and sufficient for these second species limiting orbits to be critical. This is a very pleasant result since, 1) it verifies the general prediction that extrema of C should be critical orbits, 2) it provides a strong check that all the computations are correct.

Finally, the multiplicative factors s_η and ρ vanish only at the points with integer coordinates $\tau/\pi = i$, $\eta/\pi = j$ with $\sigma =$

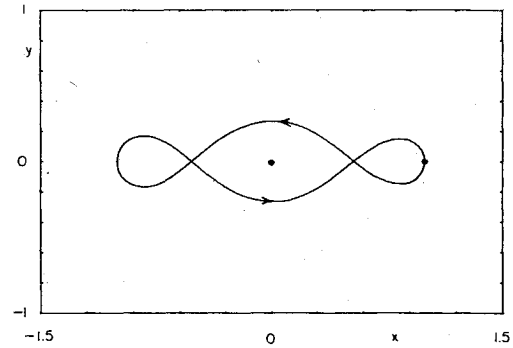

Fig. 10 The first critical second species limiting orbit $C_{12}(1)$. This is a direct orbit in fixed axes.

Table 1 Critical second species orbits for $\mu = 0$, parameters for the six orbits shown in Figs. 10-15

Name	Fig. no.	n^*	τ/π	η/π	σ_0	σ_1	σ_2	a	e	x_0	x_1	C	T
$C_{12}(1)$	10	3	0.98725	1.97522	+	+	−	0.63289	0.58182	−1.00112	0.26466	2.87412	6.20310
$C_{23}(1)$	11	2	1.99451	2.99244	−	+	+	0.76343	0.30997	−0.52679	1.00007	2.97130	12.53191
$C_{24}(2)$	12	6	2.12158	3.77226	−	−	−	0.69628	0.57791	1.09867	−0.29389	0.07423	13.33030
$C_{25}(1)$	13	4	1.99366	4.97863	−	+	+	0.54459	0.83813	−0.08815	1.00103	2.64132	12.52652
$C_{38}(1)$	14	7	2.99629	7.98179	+	+	−	0.52112	0.92046	−1.00078	0.04145	2.48322	18.82627
$C_{38}(2)$	15	11	3.01234	7.94148	+	−	−	0.52636	0.91527	−1.00812	0.04460	1.31530	18.92711

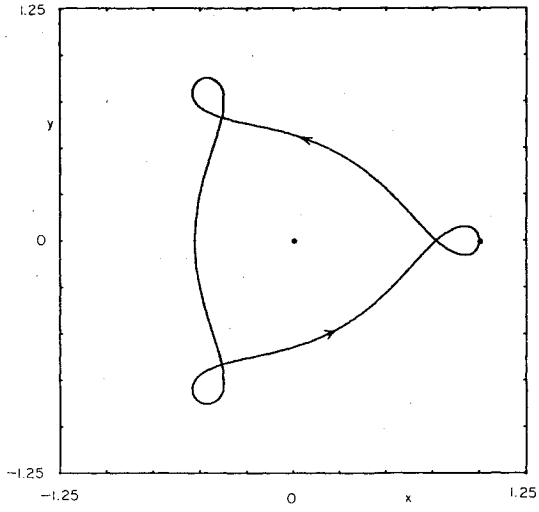

Fig. 11 The critical second species limiting orbit $C_{23}(1)$. This is again a direct orbit in fixed axes.

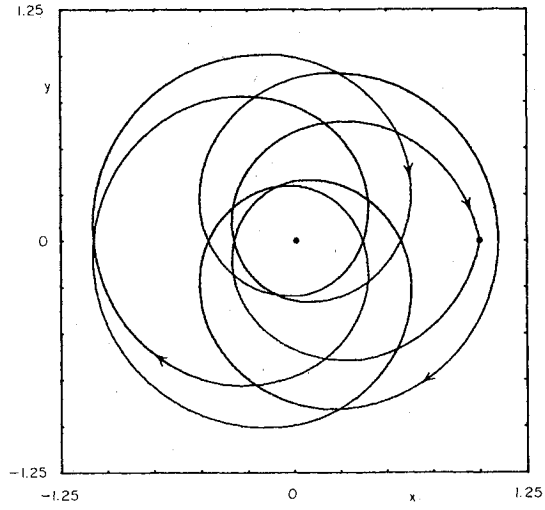

Fig. 12 The second critical generating orbit $C_{24}(2)$. This is a retrograde orbit.

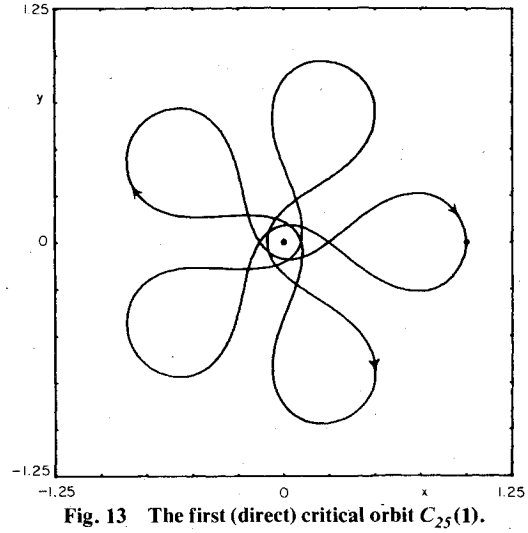

Fig. 13 The first (direct) critical orbit $C_{25}(1)$.

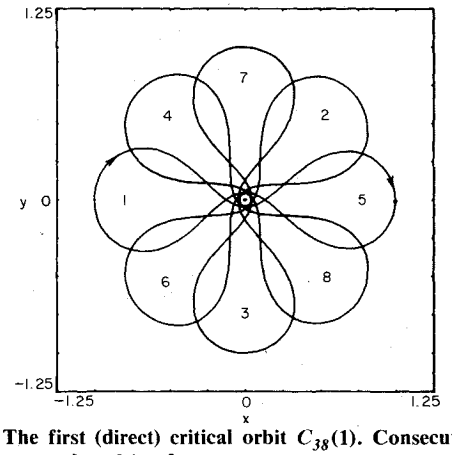

Fig. 14 The first (direct) critical orbit $C_{38}(1)$. Consecutive orbital passages are numbered 1 to 8.

$(-1)^{i+j}$. However, as explained elsewhere,[14] we find the condition $G=0$ given by Eq. (29) is meaningless at these points. Consequently, these factors indeed introduce no extraneous solutions.

Illustrations

In order to illustrate the variety of critical second species orbits which are now accessible, plots for six of these orbits are shown in Figs. 10-15. These orbits, which all belong to the families C_{ij}, are quite interesting since, as shown in Figs. 13-15, they can also have rather close passages by the Earth. Pertinent data for these six orbits are listed in Table 1. The quantity n^* is simply one-half the number of intersections of the orbit with the x axis during one orbit period $T=2\tau$. If $n^*=1$, the orbit is termed simple-periodic, $n^*=2$ is called double-periodic, etc. The inertial position of the particle at $t=E=0$ is given by x_0 with

$$x_0=\sigma_0 a(\sigma_2-e) \tag{42}$$

from Eq. (18), while the other perpendicular crossing x_1 (in fixed coordinates) occurs at $E=\pi$ so

$$x_1=-\sigma_0 a(\sigma_2+e) \tag{43}$$

Also, the direct orbits $C_{ij}(1)$ all occur at maxima of C whereas all of the retrograde orbits $C_{ij}(2)$ occur at minima of C. Finally, each orbit is symmetrical with respect to the x axis and has one orthogonal crossing of this axis and one intersection with the Moon at a so-called "angular point." These "angular points" are simply the second species limit for the local hyperbolic motion in the neighborhood of the Moon. The deflection angle δ is zero, in fact, only for orbits with integer values for τ/π and η/π.

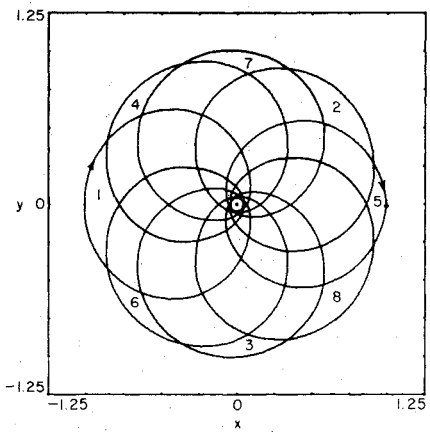

Fig. 15 The second (retrograde) critical orbit $C_{38}(2)$. Consecutive orbital passages are numbered 1 to 8.

Acknowledgment

It is a pleasure to acknowledge the major contributions of: K. L. Remmler, who initially suggested the problem of stability of periodic orbits; J.V. Breakwell, who has shared his results on the stability analysis of periodic orbits with me for a number of years; M. Hénon, who has collaborated in the study of these orbits during the last year by means of an invaluable, and extended, correspondence.

References

[1] Perko, L.M., "Periodic Orbits in the Restricted Three-Body Problem: Existence and Asymptotic Approximation," *SIAM Journal of Applied Mathematics,* Vol. 27, July 1974, pp. 200-237.

[2] Arenstorf, R.F., "Periodic Solutions of the Restricted Three-Body Problem Representing Analytic Continuations of Keplerian Elliptic Motions," *American Journal of Mathematics,* Vol. 85, Jan. 1963, pp. 27-35; also NASA TN D-1859.

[3] Broucke, R.A., "Periodic Orbits in the Restricted Three-Body Problem with Earth-Moon Masses," Jet Propulsion Laboratory, TR 32-1168, 1968.

[4] Hénon, M., "Exploration Numérique du Probleme Restreint II. Masses Égales, Stabilité des Orbites Périodiques," *Annales d' Astrophysique,* Vol. 28, 1965, pp. 992-1007.

[5] Abraham, R., *Foundations of Mechanics,* W.A. Benjamin, Inc., New York, 1967, pp. 219-230.

[6] Breakwell, J.V. and Perko, L.M., "Second-Order Matching in the Restricted Three-Body Problem (Small μ)," *Celestial Mechanics,* Vol. 9, July 1974, pp. 437-450.

[7] Fehlberg, E., "Runge-Kutta Type Formulas of High-Order Accuracy and Their Application to the Numerical Integration of the Restricted Problem of Three Bodies," *Proceedings of the International Symposium on Analogue and Digital Techniques Applied to Aeronautics,* 1963, Liège, Belgium, pp. 351-359.

[8] Fehlberg, E., "New One-Step Integration Methods of High-Order Accuracy Applied to Some Problems in Celestial Mechanics," NASA TR R-248, 1966.

[9] Darwin, G.H., "Periodic Orbits," *Scientific Papers,* Vol. IV, Cambridge University Press, 1911.

[10] Szebehely, V., *Theory of Orbits,* Academic Press, New York, 1967.

[11] Hénon, M. and Guyot, M., "Stability of Periodic Orbits in the Restricted Problem," *Periodic Orbits, Stability, and Resonances,* edited by G.E.O. Giacaglia, D. Reidel Publishing Co., Dordrecht, 1970, pp. 349-374.

[12] Hénon, M., "Sur Les Orbites Interplanétaires Qui Rencontrent Deux Fois La Terre," *Bulletin Astronomique,* Vol. 3, 1968, pp. 377-402.

[13] Poincaré, H., *Méthodes Nouvelles de la Mécanique Céleste,* Gauthier-Villars, Paris, 1892; also Dover Publications, New York, 1957 and NASA TT F-452, 1967.

[14] Hitzl, D.L. and Hénon, M., "Critical Generating Orbits for Second Species Periodic Solutions of the Restricted Problem," *Celestial Mechanics,* to appear.

[15] Breakwell, J.V., private communication to L.M. Perko and D.L. Hitzl, 1970.

[16] Hitzl, D.L. and Hénon, M., "The Stability (for $\mu = 0$) of Second Species Periodic Orbits in the Restricted Problem," *27th IAF Congress,* 1976; *Acta Astronautica,* to appear.